



Prediction of the interfacial shear-stress in vertical annular flow

R.J. Belt, J.M.C. Van't Westende, L.M. Portela *

Multi-Scale Physics Department, J.M. Burgerscentrum for Fluid Mechanics, Delft University of Technology, Prins Bernhardlaan 6, 2628 BW Delft, The Netherlands

ARTICLE INFO

Article history:

Received 26 September 2008
 Received in revised form 19 December 2008
 Accepted 30 December 2008
 Available online 12 January 2009

Keywords:

Vertical annular flow
 Interfacial friction
 Roll waves
 Interfacial sand-grain roughness

ABSTRACT

Many improvements of the Wallis correlation for the interfacial friction in annular flow have been proposed in the literature. These improvements give in general a better fit to data, however, their physical basis is not always justified. In this work, we present a physical approach to predict the interfacial shear-stress, based on the theory on roughness in single-phase turbulent pipe flows. Using measured interfacial shear-stress data and measured data on roll waves, which provide most of the contribution to the liquid film roughness, we show that the interfacial shear-stress in vertical annular flow is in very close agreement with the theory. We show that the sand-grain roughness of the liquid film is not equal to four times the mean film thickness, as it is assumed in the Wallis correlation. Instead, the sand-grain roughness is proportional to the wave height, and the proportionality constant can be predicted accurately using the roughness density (or solidity). Furthermore, we show that our annular flow, which is in similar conditions to others in the literature, is fully rough. Hence, the bulk Reynolds number should not appear in the prediction of the interfacial friction coefficient, as is often done in the improvements of the Wallis correlation proposed in the literature.

© 2009 Elsevier Ltd. All rights reserved.

1. Introduction

Annular flow is a two-phase flow configuration which often occurs in pipes used for the production and transport of gas. In annular flow, the liquid (e.g., gas condensates or oil) flows partly as a thin and wavy film along the wall, and partly as droplets entrained in the turbulent gas core. To improve the production processes and the separation of the two phases, it is required to predict accurately the phase distribution in the pipe. This prediction, using the continuity and force balances on the film and the gas core, requires an estimate of the interfacial shear-stress. Indeed, the drag on the interface is one of the largest forces in the force balances, and it promotes the coupling between the wavy film and the turbulent gas core. In this work, we focus on the prediction of the interfacial shear-stress in vertical annular flow.

It has been observed that the roll waves on the interface have a large contribution to the interfacial friction (see Wallis, 1969). The roll waves are large waves which are coherent over long distances (see, e.g., Azzopardi, 1997), and which are randomly distributed in space (see Belt, 2007; Belt et al., 2007). Therefore, the film can be seen as a rigid and rough wall from the perspective of the gas flow. In the literature, a number of correlations have been proposed for the interfacial friction which are more or less based on the analogy with the friction in turbulent pipe flows due to rough walls (Wallis, 1969; Henstock and Hanratty, 1976; Asali et al., 1985; Fore et al., 2000). The first correlation for the interfacial friction was proposed

by Wallis (1969); it uses an analogy to a simplified form of the friction correlation in fully rough pipes, valid over a small range of roughness. Over the years, the Wallis correlation has been modified in order to match the experimental results over a larger range of film thickness. The modifications consist mostly of: (i) small changes in the form and in the constants of the Wallis correlation, and (ii) the inclusion of a Reynolds number dependency. According to Fore et al. (2000), and Lopes and Dukler (1986), the introduction of a Reynolds number dependency could be justified by the occurrence of transition roughness, instead of full roughness. However, no physically based justification was given for this suggestion. Also, it is not clear from their work how transition roughness should be implemented correctly in the correlation.

In this work, we discuss the modifications of the Wallis correlation proposed in the literature, and propose an extension which is more physically based. First, we briefly present the theory on roughness in turbulent pipe flows, and how this has been applied (with its limitations) to vertical annular flow. Next, we explain how the interfacial friction is obtained experimentally in vertical annular flow and we compare our experimental results to existing interfacial friction correlations for vertical annular flow. Finally, we show the limitations of the existing correlations, and we propose a more physical approach to obtain the interfacial friction, based on our experimental data.

2. Roughness in turbulent pipe flows

Roughness in single-phase turbulent pipe flows has been studied extensively (see, e.g., Schlichting, 1979; Pope, 2000; or Jimenez,

* Corresponding author.

E-mail address: L.Portela@tudelft.nl (L.M. Portela).

2004). From dimensional analysis, it can be shown that in the wall region dominated by the inertial scales, the mean velocity profile $U(y)$ is logarithmic, similarly to single-phase flow in a pipe with smooth walls; this can be expressed as:

$$U^+(y) = \frac{1}{\kappa} \ln \left(\frac{y}{k_s^+} \right) + B' (k_s^+) \quad (1)$$

where the superscript + denotes the values in wall units (i.e., made dimensionless with the kinematic viscosity ν_G and the friction velocity $u_\tau = (\tau/\rho_G)^{0.5}$, where τ is the wall shear-stress, and ρ_G the density), y is the distance from the wall, k_s the sand-grain roughness, which is a typical length scale of the roughness elements, κ the von Karman constant and B' an additive constant depending on k_s^+ . We note that, in principle, the logarithmic velocity profile is only valid in the log-law region, i.e., $y^+ \geq 30$ and $y/D \leq 0.3$, with D the pipe diameter. However, in practice, the deviations from the log-law in the central part of the pipe are small.

In general, the additive constant B' is a function of the ratio between the viscous scales and the scales of the roughness elements k_s . However, for large roughness scales, the pressure forces on the roughness elements become dominant over the viscous forces, and, on dimensional grounds, the additive constant B' should become a constant. In practice, B' becomes equal to 8.5 for $k_s^+ \geq 70$ –100, which is denoted as the fully rough regime. The mean velocity profile in Eq. (1) can also be expressed in terms of the log-law for smooth walls, when including an offset ΔU^+ :

$$U^+(y) = \frac{1}{\kappa} \ln (y^+) + B - \Delta U^+ \quad (2)$$

where B is the smooth wall log-law intercept, and ΔU^+ the roughness function, which is a function of the sand-grain roughness k_s . With the log-law for fully rough pipes written in the form of Eq. (2), we clearly see that ΔU^+ , or equivalently k_s , represents the extra drag due to roughness, when compared to smooth walls. This also means that the sand-grain roughness k_s is a hydrodynamic representation of the dimensions of the roughness elements, related to the drag, and must be related to the size of the roughness elements before it can be used (see Jimenez, 2004).

Assuming the log-law to be valid in the central part of the pipe, for the fully rough regime, the friction factor C_f , defined as $C_f = \tau/(\rho_G U_B^2)$, with U_B being the bulk velocity, can be derived directly from Eq. (1); it can be expressed as:

$$C_f = \frac{1}{8} \left(1.74 + 2.0 \log \left(\frac{D}{2k_s} \right) \right)^{-2} \quad (3)$$

with the constants 1.74 and 2.0 instead of 1.71 and 1.99, respectively, which would result from the derivation. These constants were proposed by Schlichting (1979) to better match the experimental results, because of the small deviations from the log-law in the central part of the pipe. From Eq. (3), we clearly see that in the fully rough regime the friction factor C_f is only a function of the sand-grain roughness k_s .

In the next section, we show how the theory on roughness can be applied to vertical annular flow.

3. Roughness in vertical annular flow

In vertical annular flow, the interface has a wavy structure. Mainly two types of waves exist on the interface: (i) ripple waves of small amplitude, and (ii) large roll waves, which are axially coherent over long distances and flow with an approximately constant wave velocity C_W (see, e.g., Azzopardi, 1997). Furthermore, it appears that the roll waves are randomly distributed in space (see Belt, 2007; Belt et al., 2007, submitted for publication). Since the amplitude of the roll waves is much larger than that of the ripple

waves, the effect of the roll waves on the interaction between the film and the gas flow is expected to be dominant over that of the ripple waves. Furthermore, due to the large density ratio between the two phases (for low-pressure air–water conditions, as in our laboratory experiments), the inertia of the turbulent fluctuations in the gas does not have a significant effect on the interfacial structure, which can explain the coherence of the roll waves.

Using these considerations, from the perspective of the gas flow, the film can be seen as a rigid and rough wall moving with the velocity $-(U_B - U_i)$, where U_i is the velocity of the interface in the reference frame of the laboratory, and U_B is the bulk velocity of the gas. Since we assume that the roll waves have the largest contribution to the interfacial friction, the velocity of the interface can be taken equal to the velocity of the roll waves C_W . Therefore, using the definition of the friction factor $\tilde{C}_{f,i}$,

$$\tilde{C}_{f,i} = \frac{\tau_i}{\rho_G (U_B - C_W)^2}, \quad (4)$$

a priori, the interfacial shear-stress τ_i can be predicted from the standard correlations of the friction factor for turbulent flow in rough pipes (e.g., the generalized Churchill, the Colebrook and White, or Haaland correlations, in the case transition roughness can play a role). This definition of the interfacial friction factor will be used below, unless otherwise stated. We note that, in the literature on annular flow, often a different definition of the interfacial friction factor is used, in which the velocity of the interface is neglected compared to the bulk velocity U_B (and which will be denoted here by $C_{f,i}$, without the tilde referring to the wave velocity, and where $C_{f,i} = \tau_i/(\rho_G U_B^2)$). However, C_W should be included in the definition of the interfacial friction factor, since: (i) the shear in the gas phase is clearly related to $U_B - C_W$ and not to U_B , and (ii) the inertia term in the denominator of Eq. (4) will be overpredicted by 10–17%, based on our experiments, when C_W is neglected.

For vertical annular flow, Wallis (1969) suggested a correlation for the interfacial friction factor $C_{f,i}$, with an analogy to full roughness. In this correlation, the interfacial friction factor is a linear function of the mean film thickness δ :

$$C_{f,i} = 0.0025 \left(1 + 300 \frac{\delta}{D} \right) \quad (5)$$

This correlation corresponds to a linear fit of the friction factor for fully rough pipes (Eq. (3)), assuming that the sand-grain roughness k_s equals four times the mean film thickness δ , and the ratio k_s/D is less than approximately 0.03 (see Wallis, 1969).

Although the Wallis correlation is widely used for engineering purposes, it has been modified over the years to yield a better match to the experimental values of the interfacial friction factor, in the limit of both thick and thin films. The corrections consist mostly of the inclusion into Eq. (5) of: (i) the gas bulk Reynolds number, and (ii) an offset in the ratio δ/D (see, e.g., Asali et al., 1985; Fore et al., 2000). The appearance of the gas bulk Reynolds number could be justified, according to Lopes and Dukler (1986) and Fore et al. (2000), by the occurrence of transition roughness, instead of full roughness, which was the basis of the Wallis correlation. However, no fundamental proofs were given for this suggestion. The other assumptions made in the Wallis correlation, i.e., the range of the validity of the fit ($k_s/D \leq 0.03$) and the relation between the sand-grain roughness k_s and the mean film thickness δ are generally not questioned.

4. Experimental determination of the interfacial friction

For a vertical annular flow, the interfacial shear-stress τ_i can be derived from the momentum balance in the axial direction of the droplet-laden gas core, without requiring a value for the

sand-grain roughness. Consequently, the interfacial friction factor $\bar{C}_{f,i}$ can be calculated.

The momentum balance in the axial direction of the gas core is given by (see Fore and Dukler, 1995a):

$$-\frac{dP}{dz} - (\alpha\rho_G + (1 - \alpha)\rho_L)g - \tau_i \frac{4}{D - 2\delta} + (R_A C_W - R_D V_D) \frac{4}{D - 2\delta} = 0 \tag{6}$$

where $-dP/dz$ is the pressure-gradient, α the void-fraction in the gas core, δ the mean film thickness, R_A and R_D the atomization and deposition rates of droplets from and onto the film, respectively, and V_D the centerline velocity of the droplets. The first term in Eq. (6) represents the driving force of the flow, the second term the gravitational forces on the gas core, the third term the transfer of momentum to the film, and the fourth term the advection of momentum due to the atomization of slow-moving droplets from the film and the deposition of fast-moving droplets back onto the film.

In Eq. (6), the pressure-gradient $-dP/dz$, the film thickness δ and the wave velocity C_W are obtained from our measurements, which are presented in Belt (2007) and Belt et al. (2007, submitted for publication) and which are summarized in Appendix A. These measurements were performed in an air/water vertical annular flow in a pipe of 0.05 m diameter, at atmospheric pressure. The flow at the measurement location is assumed fully developed, since the measurements were performed 130 pipe diameters downstream the porous wall water inlet (in agreement with e.g., Wolf et al., 2001). Furthermore, we measured the mean axial pressure-gradient between 80D and 140D and between 120D and 140D. The differences are smaller than the measurement error, meaning that the annular flow is developed as far as the mean axial pressure-gradient is concerned. The measurements were made in the annular flow regime without flow reversal, i.e., above or at the minimum of the pressure-gradient (see Zabarás et al., 1986). The gas superficial velocity U_{GS} covers a range between 22 and 42 m/s, while the liquid superficial velocity U_{LS} is between 0.01 and 0.08 m/s (see Table 1). In our work, the void-fraction in the gas core α , the atomization and deposition rates R_A and R_D , and the centerline velocity of the droplets V_D , were not measured and must be estimated correctly.

For instance, R_A , R_D and V_D must be estimated accurately, since the loss of momentum due to entrainment and deposition of droplets can account for approximately 20% of the pressure-gradient, as shown in Fore and Dukler (1995a). First, we assume that our annular flow is developed, therefore, R_A and R_D are equal, due to continuity. The value of the deposition rate R_D is obtained from interpolation of the experimental results presented in Fore and Dukler (1995a), who studied a vertical annular flow in conditions similar to ours. The centerline velocity of the droplets V_D is set in our work equal to the gas bulk velocity U_B , which is a good estimate according to the data in Fore and Dukler (1995a,b) and Van't Westende et al. (2007). We note that changing V_D from $0.8 \cdot U_B$ to $1.2 \cdot U_B$ does not change the overall picture presented below. The

Table 1

Gas and liquid superficial velocities, U_{GS} and U_{LS} , respectively, in our measurements. Values for the superficial velocities are in m/s. Re_{GS} and Re_{LS} are the Reynolds numbers based on the pipe diameter and the gas and liquid superficial velocity, respectively. We note that the values of the gas superficial velocities can vary by a maximum of 0.3 m/s around the values in the table, at the different values of U_{LS} .

U_{GS}	21.9	26.2	31.0	36.4	42.1
Re_{GS}	75×10^3	89×10^3	106×10^3	124×10^3	143×10^3
U_{LS}	9.6×10^{-3}	1.9×10^{-2}	4.0×10^{-2}	8.2×10^{-2}	
Re_{LS}	431	855	1805	3705	

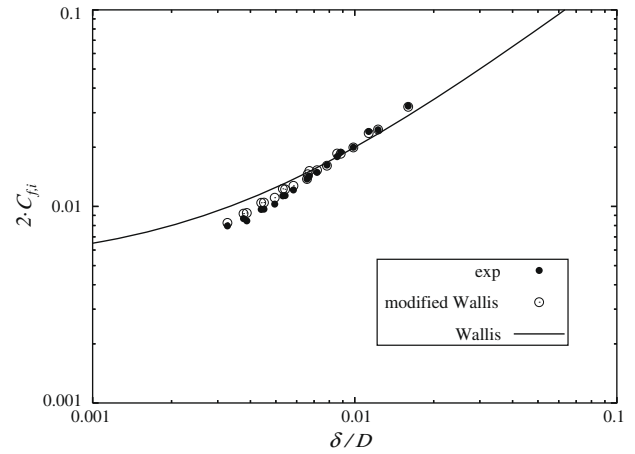


Fig. 1. Comparison of the interfacial friction factor $C_{f,i}$ derived from our experiments (solid dots) with the Wallis correlation (line) and with the modified Wallis correlation as proposed by Fore et al. (2000) (open dots).

gravitational forces in the momentum balance are small compared to the other terms, since they represent at maximum 3.5% of the mean axial pressure-gradient. Therefore, the void-fraction in the gas core α will not play a large role in the momentum balance. Its value is obtained from interpolation of the data on entrainment presented in Fore and Dukler (1995a).

The friction factor $C_{f,i}$ obtained from the momentum balance, as defined in the previous section (similarly to Fore et al., 2000), is shown in Fig. 1. It is shown together with the Wallis correlation and the modified Wallis correlation proposed by Fore et al. (2000), which is fitted to a large set of data on annular flow. From Fig. 1, we can see that the interfacial friction factor $C_{f,i}$ derived from our measurements agrees very well with the modified Wallis correlation. The difference is less than 25%, which is the scatter between the modified Wallis correlation and the data sets used in its fit. This suggests that our experimental data is in agreement with the other data sets in the literature, and that our vertical annular flow is correctly developed.

We can see that the Wallis correlation tends to under-predict the interfacial friction factor $C_{f,i}$ for a large film thickness ($\delta/D \geq 0.02$) and to over-predict for a small film thickness ($\delta/D \leq 0.005$), in agreement with the findings in other works (see, e.g., Fore et al., 2000). The difference can be explained partly due to the fact that the correlation of Wallis (see Wallis, 1969) is based on a fit of the interfacial friction factor calculated from the total pressure-gradient, and not from the total pressure-gradient reduced by the advection of momentum due to the droplets. The mechanism of transfer of momentum by the advection of droplets was proposed later by Lopes and Dukler (1986) and Fore and Dukler (1995a), and it can be relatively important (i.e., it can equal as much as 20% of the total pressure-gradient, see Fore and Dukler, 1995a). Therefore, the interfacial friction factor calculated from the Wallis correlation tends to an over-prediction, as it is observed for thin films. For thick films, the difference between the experimental results and the Wallis correlation is explained in the next sections.

Furthermore, we see that the interfacial shear-stress can be described by a function of the film thickness δ only, although the experimental results are obtained from experiments conducted at different gas bulk velocities. Since the roughness height of the film is a function of the mean film thickness δ , as we will see below, the interfacial friction factor can be described with a characterization of the roughness only. This suggests that the roughness is in the fully rough regime, and the Reynolds number of the gas flow is not a parameter of the problem. Consequently, the Reynolds

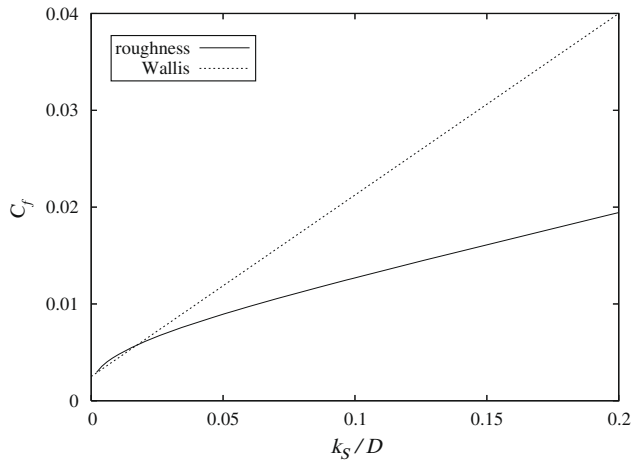


Fig. 2. Comparison of the linear fit of the friction factor for fully rough pipes, used in the Wallis correlation, with the actual friction factor for fully rough pipes, for the range of sand-grain roughness in the experiments.

number should not be included in the correlation of the interfacial friction factor.

Another problem with the Wallis correlation is that it is based on a linear fit of the friction factor for turbulent flow in fully rough pipes (Eq. (3)), and on the assumption that the sand-grain roughness is equal to four times the mean film thickness. In Fig. 2, we compare the actual friction factor for fully rough pipes (Eq. (3)) with the linear fit used in the Wallis correlation, i.e., with $k_s = 4 \cdot \delta$, for the range of sand-grain roughness found in the experiments (given below). Obviously, the friction factor based on the Wallis correlation can produce a correct estimation for $k_s/D \lesssim 0.025$, but over-predicts by up to a factor of two the actual friction factor for a large part of the range of sand-grain roughness found in our experiments.

Based on these results, to extend the Wallis correlation, we propose to use the existing correlations for roughness in single-phase turbulent pipe flows, which are valid over a large range of sand-grain roughness, and to use a more accurate estimate of the sand-grain roughness k_s . This is developed in the next section.

5. Correlation for the sand-grain roughness and interfacial friction factor

The correlations of the friction factor in rough pipes are, among others, a function of the sand-grain roughness k_s , which characterizes the drag due to the roughness elements. However, before the sand-grain roughness can be used in predictions, it must be related to the surface geometry (see Jimenez, 2004).

From the experimental values of the interfacial shear-stress τ_i , the corresponding sand-grain roughness k_s can be computed using a standard relation for the friction factor. Here, we use the generalized Churchill correlation (see Churchill, 1977):

$$\tilde{c}_{f,i} = \left(\left(\frac{8}{Re_B} \right)^{12} + \frac{1}{(c_1 + c_2)^{3/2}} \right)^{1/12} \quad (7)$$

$$c_1 = \left(2.457 \cdot \ln \left(\left(\frac{7}{Re_B} \right)^{0.9} + 0.27 \frac{k_s}{D - 2\delta} \right) \right)^{16} \quad (8)$$

$$c_2 = \left(\frac{37530}{Re_B} \right)^{16} \quad (9)$$

where Re_B is the bulk Reynolds number, based on the relative mean gas velocity in the gas core $U_B - U_i$ (with U_i taken equal to the roll wave velocity C_w , since the roll waves are assumed to have the largest contribution to the interfacial friction) and on the gas core diam-

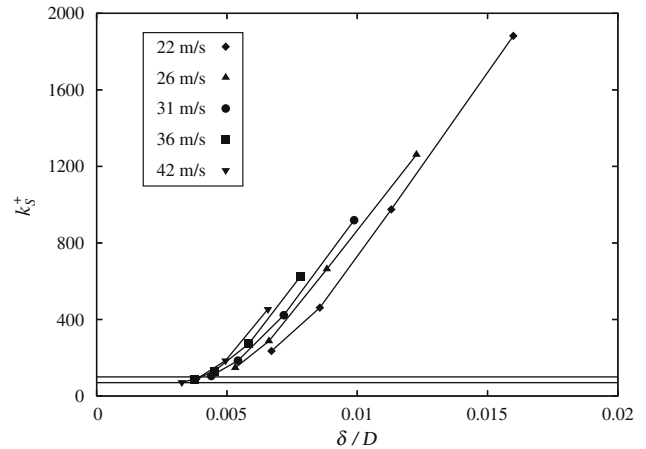


Fig. 3. Sand-grain roughness (in wall units) as a function of the film thickness δ . The two horizontal lines correspond to 70 and 100 wall units, which is the limit above which the roughness is fully developed. Each curve connecting the dots corresponds to one gas superficial velocity U_{CS} . The velocities near the dots indicate the values of U_{CS} .

eter $D - 2\delta$. We note that the generalized Churchill correlation is valid for the K-type of roughness, i.e., the “normal rough surfaces”, for which the sand-grain roughness k_s becomes proportional to the dimensions of the roughness elements in the limit of very-large roughness (when viscous effects become negligible). We note that the generalized Churchill correlation is also valid in the transition regime.

The computed sand-grain roughness is shown in Fig. 3, in wall units (i.e., normalized by the friction velocity $u_{\tau,i} = (\tau_i/\rho_G)^{0.5}$ and the gas kinematic viscosity ν_G), as a function of the film thickness δ . Fig. 3 shows that, for the majority of the measurements, k_s^+ is larger than 70–100 wall units, which represents the limit above which the roughness is in the fully rough regime. In the experiments of Fore and Dukler (1995a), we also estimated the value of k_s^+ , using their measured film thickness, the correlation of the interfacial friction factor developed by Fore et al. (2000), which is partially based on the Fore and Dukler (1995a) data set, and a sand-grain roughness equal to four times the mean film thickness (which is an underestimation of the actual sand-grain roughness, as we will see below). In their experiments, also, the sand-grain roughness is larger than 100 wall units. This suggests that the roughness in the majority of the experiments is in the fully rough regime. Therefore, the error in the prediction of the interfacial friction factor with the original Wallis correlation has probably more to do with the shape of the fit used by Wallis than with transition roughness, as suggested by Lopes and Dukler (1986) and Fore et al. (2000). Consequently, the correction of the Wallis correlation should not include a gas Reynolds number dependence, since such a correction could completely fail when used for rather different situations (e.g., different pipe diameters or different fluids).

For K-roughness in the fully rough regime, the sand-grain roughness k_s should become proportional to the dimensions of the roughness elements. Therefore, in Fig. 4, we show the sand-grain roughness k_s (in outer units, i.e., normalized by the pipe diameter) as a function of the standard deviation of the film thickness $rms(\delta)$, which is a global measure of the film roughness. We can see that, indeed, k_s is a function of $rms(\delta)$ only, with experiments done at different gas and liquid superficial velocities U_{CS} and U_{LS} . Fig. 4 also shows that the range of k_s/D in the experiments is significantly larger than 0.025, which is approximately the limit up to which the Wallis correlation is a correct fit of the actual friction.

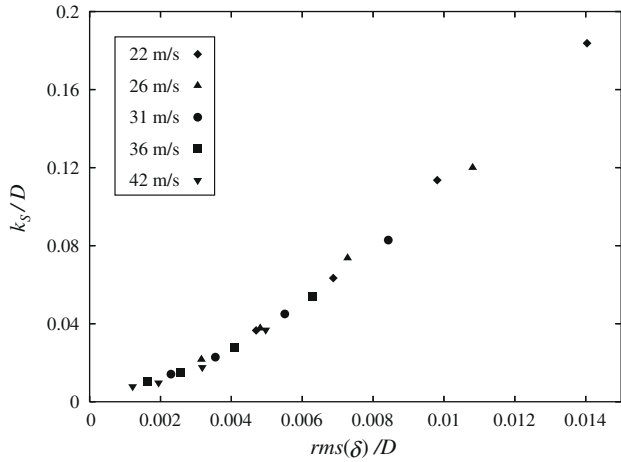


Fig. 4. Sand-grain roughness (in outer units) as a function of the standard deviation of the film thickness $rms(\delta)$, which is a global measure for the film roughness. The velocities near the dots indicate the values of the gas superficial velocity U_{CS} .

Assuming that the roughness is mostly due to the roll waves, the size of the roughness elements is mainly characterized by the roll-wave height h_w . Then, applying the approach of Schlichting (1936) and Jimenez (2004) to annular flow, the ratio k_s/h_w should be a function of the roughness density, quantified by the solidity λ (which is equal to the frontal roughness area, perpendicular to the mean flow direction, per unit of interface area projected on the plane parallel to the mean flow direction). In our experiments, the solidity λ is defined by:

$$\lambda = \frac{N_f}{C_w} \cdot h_w \quad (10)$$

where N_f is the mean frequency of the roll waves. In Fig. 5, we show the ratio k_s/h_w as a function of the solidity λ . We can see that, for $\lambda \geq 0.002$, the ratio k_s/h_w is proportional to the solidity λ . This is consistent with the results on K-roughness in single-phase turbulent pipe flows, which are presented in Jimenez (2004) and reported in Fig. 5. In a sparse regime, where the roughness elements do not

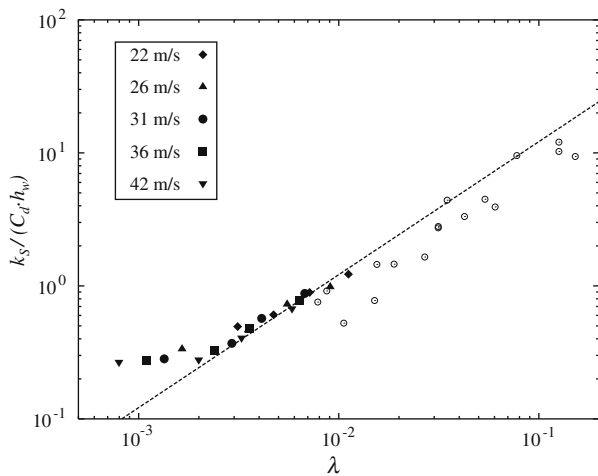


Fig. 5. Sand-grain roughness k_s as a function of the solidity λ . The drag coefficient C_d should be set to approximately 2.5 to match the results of Schlichting (see Jimenez, 2004; Schlichting, 1936). It is larger than the value of approximately 1.25 suggested by Jimenez (2004) for two-dimensional spanwise obstacles, based on the results in Tillman (1944). The line corresponds to the slope equal to unity, i.e., a linear dependence between the x and y axes. The solid dots correspond to our measurements, with the velocities near the dots indicating the values of the gas superficial velocity U_{CS} . The open dots correspond to measurements of Schlichting on “real roughness” elements, presented by Jimenez (2004).

shelter each other, the drag due to the roughness elements should be proportional to the frontal roughness area, therefore, k_s/h_w should be proportional to the solidity λ , in the fully rough regime. In Fig. 5, we also see that, for a few points for which $\lambda \leq 0.002$, the ratio k_s/h_w becomes a very-weak function of λ . For these data points, k_s^+ is close to the range of 70–100 wall units, therefore, the liquid film can be in the transition regime. These data points correspond also to the lowest superficial liquid velocity U_{LS} , for which the frequency of the waves is very low (approximately 2–3 Hz). Therefore, in between the large waves, the viscous cycle of turbulence close to the interface may not be completely disrupted, leading to the occurrence of transition roughness.

In the fully rough regime, the use of the solidity λ can give a robust modeling of the sand-grain roughness k_s , since it is proportional to the height of the roll waves, with the solidity as proportionality constant. We note that, strictly, this proportionality holds only for the fully rough regime. In the transition regime, the function k_s/h_w might depend on other parameters than only λ . Hence, at the moment the sand-grain roughness can be computed accurately with the solidity only in the fully rough regime. For most of our experimental conditions, which are similar to others in the literature, the interface is in the fully rough regime. It would be interesting to apply these ideas to annular flows with other fluids and pipe diameters, and to check whether the interface in these annular flows is also, for most conditions, in the fully rough regime.

In our experiments, the lowest gas Reynolds number is 75,000. It could be argued that transition roughness will occur for lower Reynolds numbers (smaller pipes), since in that case the physical height of the inner layer will be larger, and possibly larger than the roll-wave height. However, the interaction between the film and the gas core complicates this reasoning. Indeed, Fig. 3 shows that in our experiments the sand-grain roughness is further away from the transition regime for the lower gas superficial velocities (lower gas Reynolds numbers) and for the higher liquid superficial velocities. This can be understood if one realizes that for higher gas superficial velocities the velocity of the interface is larger, therefore, for the same liquid superficial velocity, the film becomes thinner. Moreover, at high gas superficial velocities, the entrainment of liquid in the gas core becomes larger, which tends to decrease the film thickness further. The behavior with the liquid superficial velocity is straightforward, since for high liquid superficial velocities the film is likely to be thicker, thus the top of the roll waves is more likely to be in the outer layer. As a result, in our case, the transition regime could be obtained for gas Reynolds numbers larger than those in our experiments, and liquid mass flow rates smaller than those in our experiments. Note that, after the prediction of the sand-grain roughness with the solidity, it can be verified whether the interface is fully rough, i.e., whether the predicted sand-grain roughness is larger than 70–100 wall units.

6. Pragmatic correlation for the interfacial friction factor

In practice, the behavior of the wave-frequency N_f is not well-known, therefore, the solidity cannot be easily predicted at the moment. In this section, we propose an easier to use pragmatic correlation for the interfacial friction factor.

In Fig. 4, we showed that the sand-grain roughness k_s is a function of the standard deviation of the film thickness $rms(\delta)$ only. Furthermore, in Fig. 6, we can see that the $rms(\delta)$ has a linear dependence on the mean film thickness δ . The reason for this linear dependence is not understood at the moment by the authors. However, from a pragmatic point of view, a correlation must then exist between the sand-grain roughness k_s and the mean film thickness δ , which is shown in Fig. 7, and which could be well-fitted by a power law. Therefore, the interfacial friction factor \tilde{C}_f can be described by a function of the mean film thickness δ only (see

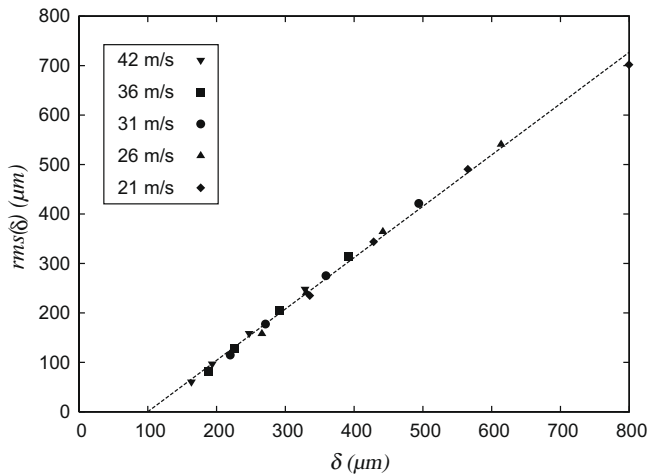


Fig. 6. Standard deviation of the film thickness $rms(\delta)$ as a function of the mean film thickness δ . The line corresponds to a linear fit to the data and its slope is equal to 1.04.

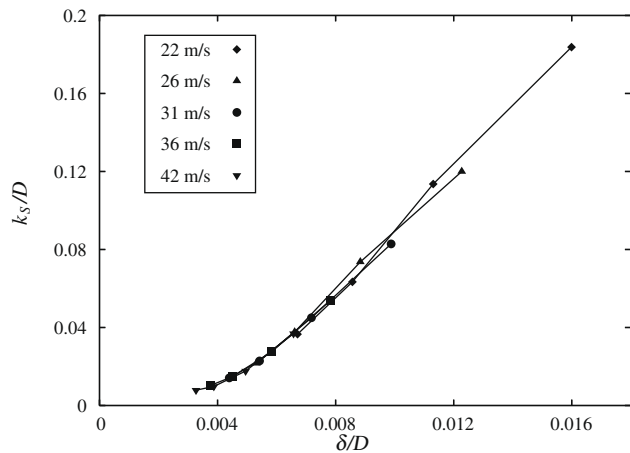


Fig. 7. Sand-grain roughness k_s as a function of the film thickness δ . Each curve connecting the dots corresponds to one superficial gas velocity U_{GS} . The velocities near the dots indicate the values of U_{GS} .

Fig. 8). From **Fig. 8**, we can see that, over the range of film thicknesses considered in our vertical annular flow, a linear dependence exists between the interfacial friction factor $\tilde{C}_{f,i}$ and the mean film thickness δ :

$$\tilde{C}_{f,i} = 1.158 \cdot \delta/D + 3.413 \times 10^{-4} \quad (11)$$

We note that this equation was obtained from the experimental data using the momentum balance of the droplet-laden gas core (i.e., no correlation for the interfacial friction factor was used), and is only valid for the range of film thickness in our water/air experiments (i.e., in the fully rough regime).

This linearity, which is also observed in the Wallis correlation, can be partly explained: for the range of sand-grain roughness k_s observed in the experiments, the friction factor for fully rough pipes can be very-well approximated by a linear relationship with the sand-grain roughness k_s (see **Fig. 2**). The departure from linearity is only observed for very-small sand-grain roughness k_s , i.e., for $k_s/D \lesssim 0.02$. Furthermore, as shown in **Fig. 7**, the sand-grain roughness k_s behaves linearly with the mean film thickness δ for $k_s/D \gtrsim 0.02$ (corresponding to $\delta/D \gtrsim 0.005$). This is due to the fully rough regime, since in this regime the sand-grain roughness is proportional to the roll-wave height, which, in turn, is approximately

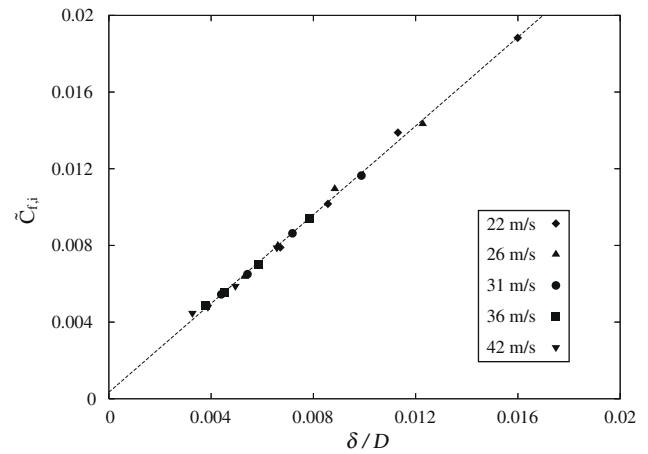


Fig. 8. Interfacial friction factor $\tilde{C}_{f,i}$ as a function of the film thickness δ . The dashed line, $\tilde{C}_{f,i} = 1.158 \cdot \delta/D + 3.413 \times 10^{-4}$, corresponds to a linear fit of the data. The velocities near the dots indicate the values of the gas superficial velocity U_{GS} .

equal to four times the mean film thickness. Then, considering both results, for $k_s/D \gtrsim 0.02$, a linear dependence must exist between the interfacial friction factor $\tilde{C}_{f,i}$ and the mean film thickness δ . Furthermore, for $k_s/D \lesssim 0.02$, the deviations from linearity are in the opposite direction between: (i) k_s and $\tilde{C}_{f,i}$, and (ii) k_s and δ , such that the relationship between $\tilde{C}_{f,i}$ and δ is still roughly linear.

We note that **Eq. (11)** results from the proportionality between the sand-grain roughness and the height of the roll waves in the fully rough regime, with the solidity as proportionality constant. Hence, the constants of the equation implicitly contain the solidity of our experiments. In other words, the equation contains the ratio of the roll-wave height and the frequency with the mean film thickness of our experiments. These ratios could be different for other fluids than air/water.

7. Validation of the sand-grain roughness

The values of the sand-grain roughness k_s found in the preceding sections are larger than the wave height, or larger than four times the film thickness δ , the value suggested by **Wallis (1969)**. To support the magnitude of the sand-grain roughness k_s found with the friction correlation of Churchill, we can determine k_s from the profiles of the mean axial gas velocity using **Eq. (1)**. Profiles of the mean axial velocity in vertical annular flow are shown in **Van't Westende et al. (2007)** for a superficial gas velocity U_{GS} of 21 m/s and superficial liquid velocities U_{LS} of 0.01, 0.02 and 0.04 m/s, which are roughly the same conditions as some results presented here.

The measured profiles of the mean axial velocity $U(y)$ are shown in **Fig. 9**. We can see that $U(y)$ shows a logarithmic behavior. This supports the suggestion that the velocity behaves as in a turbulent flow over a rough wall, and that the use of **Eqs. (1)–(3)** is justified. We note that the mean axial velocity in **Fig. 9** is not normalized by the friction velocity u_τ , which explains the different logarithmic slopes in the profiles for different conditions. Nevertheless, we can use **Eq. (1)** to determine the friction velocity u_τ from the logarithmic slope (using a von Karman constant κ equal to 0.41), and, afterwards, the sand-grain roughness k_s from the log-law intercept (using the value 8.5 for the constant B').

The sand-grain roughness k_s and the friction velocity u_τ resulting from the profiles of the mean axial gas velocity are compared in **Table 2** with k_s obtained from the Churchill friction correlation and $u_\tau = (\tau_i/\rho_G)^{0.5}$ determined in the experiments (in which the interfacial shear-stress τ_i is set here equal to $-dP/dz \cdot D/4$, with $-dP/dz$ being the measured mean axial pressure-gradient). Con-

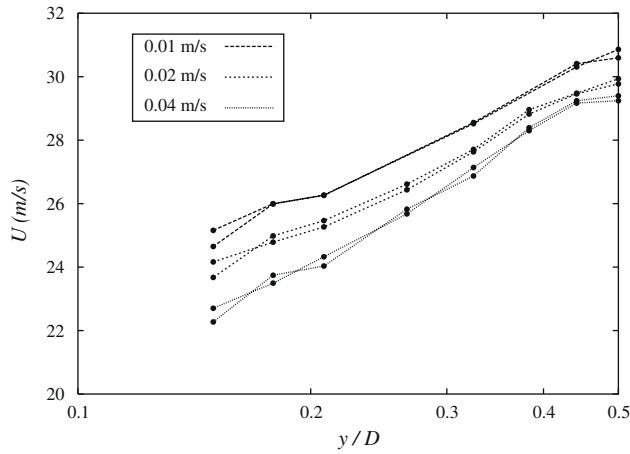


Fig. 9. Profiles of the mean axial gas velocity in vertical annular flow for different liquid superficial velocities U_{LS} at the superficial gas velocity U_{GS} of 21 m/s. The measurements are presented in Van't Westende et al. (2007). The two curves for each value of U_{LS} correspond to the profiles measured on both sides of the pipe.

Table 2

Comparison of the values of the sand-grain roughness k_S and the friction velocity u_τ obtained by the Churchill friction factor and by the profile of the mean axial gas velocity, for a superficial gas velocity U_{GS} roughly equal to 21–22 m/s.

U_{LS} (m/s)	Friction factor			Velocity profile		
	u_τ (m/s)	k_S/D	k_S/δ	u_τ (m/s)	k_S/D	k_S/δ
0.01	1.97	0.036	4.40	2.00	0.030	5.45
0.02	2.24	0.063	5.25	2.09	0.045	7.39
0.04	2.65	0.114	10.25	2.46	0.115	10.04

Considering the uncertainties in the measurement of the pressure-gradient and in the mean axial velocity profiles (which are assumed to be equal to the velocity profiles of the smallest measurable droplets of roughly 20 μm , see Van't Westende et al. (2007)), we can conclude from Table 2 that the sand-grain roughness k_S and the friction velocity u_τ obtained by both approaches are in reasonable agreement. It is also clear from Table 2 that the sand-grain roughness k_S obtained from the mean axial velocity profile is not equal to four times the mean film thickness, and that k_S is not necessarily equal to the roughness height (roll-wave height).

8. Conclusions

In vertical annular flow, the interfacial friction is often calculated using the Wallis correlation (see Wallis, 1969) or slight modifications to it (see, e.g., Fore et al., 2000). The Wallis correlation shows an analogy to the friction for single-phase turbulent flows in rough pipes. Indeed, when it is assumed that the sand-grain roughness is equal to four times the mean film thickness, the Wallis correlation corresponds to a linear fit of the friction factor for fully rough pipes for a small range of roughness. In the literature, improvements of the Wallis correlation have been proposed in order to better fit the experimental results over a larger range of vertical annular flow conditions. The modifications consist mainly of the incorporation of a gas Reynolds number, and have been explained by the existence of transition roughness, instead of full roughness. However, a physical justification for this has not been given.

In this work, the interfacial friction in vertical annular flow without flow reversal is investigated using experimental data. Our results show that, indeed, for a range of conditions which is similar to other works, the interfacial friction can be described

by the roughness theory for single-phase turbulent flows in rough pipes.

Instead of using a “curve fit”, we applied the formulation of the friction factor for single-phase turbulent flows in rough pipes (for example, the Churchill relation) to vertical annular flow without flow reversal. In this formulation, the friction is a function of the sand-grain roughness k_S , which is a characteristic length scale of the roughness effects, and which must be related to the dimensions of the roughness elements k (in our case the height of the roll waves). Our results show that, in the fully rough regime, the sand-grain roughness is proportional (but not necessarily equal) to the height of the roll waves. The proportionality constant can be predicted accurately using the roughness density, or “solidity” (see Schlichting, 1936; Jimenez, 2004). Moreover, the proportionality constant in vertical annular flow is in good agreement with that for single-phase turbulent flows in rough pipes. We also calculated the sand-grain roughness from the axial velocity profile in the gas core. The mean gas axial velocity profile shows a logarithmic behavior, similar to that in single-phase turbulent flows in rough pipes, and provides a sand-grain roughness in good agreement with that found using the Churchill relation and the solidity. We note that the proportionality between the sand-grain roughness and the roll-wave height, with the solidity as proportionality constant, holds, strictly, only for the fully rough regime. For most of our experimental conditions, which are similar to others in the literature, the interface is in the fully rough regime. It would be interesting to apply these ideas to annular flows with other fluids and pipe diameters, and to check whether the interface in these annular flows is also, for most conditions, in the fully rough regime (note that, after the prediction of the sand-grain roughness using the solidity, it can be verified whether the interface is fully rough, i.e., whether the predicted sand-grain roughness is larger than 70–100 wall units). As a future work, it would be interesting to verify our ideas on annular flows with other fluids or pipe diameters, however, we emphasize that in order to do this we need to know many parameters: the mean axial pressure-gradient, the atomization rate, the mean film thickness, the void-fraction in the gas core, and the velocity, height and frequency of the roll waves.

Our results show that the interface of our vertical annular flow is in the fully rough regime. Therefore, the interfacial friction can be described by the dimensions of the roll waves only, and the gas Reynolds number should not be included. However, the modifications of the Wallis correlation often contain the gas Reynolds number. Therefore, we wonder whether such a correction is appropriate. The original Wallis correlation is based on the fully rough regime, although it predicts values for the interfacial friction slightly different from the experimental ones in the limit of thin and thick films. We showed that the differences obtained with the Wallis correlation can be explained by: (i) a too small region where its fit to the friction factor for fully rough pipes is valid, (ii) a sand-grain roughness different from four times the mean film thickness, (iii) the neglect of the interfacial velocity in the definition of the interfacial friction factor, and (iv) a fit based on uncorrected interfacial shear-stress data, since the data used by Wallis (1969) were not corrected for the advection of momentum due to the droplets (and which is not negligible, see Fore and Dukler (1995a) or Lopes and Dukler (1986)).

In practice, the roughness density cannot be easily predicted, since it involves quantities such as the frequency and the height of the roll waves. Therefore, the prediction of the interfacial friction using the solidity requires more knowledge on the stability, formation and dynamics of the roll waves. We also propose, like Wallis (1969), a straightforward relation, found experimentally, between the interfacial friction factor and the mean film thickness, for the fully rough regime. This pragmatic relation results from the simple relations between the interfacial friction factor, the sand-grain

roughness, the characteristic height of the waves and the mean film thickness. In particular, it is based on the linear relationship between the sand-grain roughness and the height of the roll waves in the fully rough regime, with the solidity as proportionality constant. We note that the constants in this pragmatic relation implicitly contain the solidity of our experiments in air/water. In other words, the relation contains the ratio of the roll-wave height and the frequency with the mean film thickness, which could be different for other fluids.

Appendix A. Vertical annular flow data

The interfacial friction is determined from our experiments in an air/water vertical annular flow at atmospheric pressure in a pipe of 0.05 m diameter and 12 m length. The experimental set-up, the measurement techniques and the statistical properties of the film, especially of the roll waves, are presented in Belt (2007) and Belt et al. (submitted for publication). Below, we summarize the main results, which are used here for the determination of the interfacial friction, together with the film thickness measurement technique.

The film thickness is measured 6.5 m (130D) downstream the water inlet, leaving sufficient distance for the liquid film to develop. The film thickness measurement technique is based on the instantaneous conductance of the liquid film, which is a function of the instantaneous film thickness. Such a technique has been widely used in the literature (see, e.g., Asali et al., 1985; Zabaras et al., 1986; Fore and Dukler, 1995a). The film thickness sensor consists of 10 measurement locations in the axial direction times 32 measurement locations in the circumferential direction, giving in total 320 measurement locations, and therefore a spatial reconstruction of the film. The time resolution is 5000 Hz for each measurement location, i.e., much higher than the phenomena observed in annular flow. The film thickness sensor is non-intrusive: the conductance at one position is measured between two electrodes flush with the wall. The separation distance between two adjacent electrodes is 6×10^{-3} m in the axial direction. This separation distance dictates the maximum film thickness which can be measured with this sensor, and is equal to about 3.5×10^{-3} m. Finally, the accuracy (twice the standard deviation) of the film thickness obtained with this sensor is about 12% of the film thickness.

The mean axial pressure-gradient in the vertical annular flow is measured using a manometer between 4 m (80D) and 7 m (140D) downstream of the water inlet. The values are shown in Fig. 10. The measurement of the mean axial pressure-gradient between 120D and 140D gives the same values, indicating that the vertical annular flow is developed as far as the mean axial pressure-gradient is concerned. In this study, we consider the results in the annular flow regime without flow reversal, i.e., the gas superficial velocities are higher or equal to that at the minimum of the mean axial pressure-gradient shown in Fig. 10. The gas superficial velocity U_{GS} is in between 22 and 42 m/s, while the liquid superficial velocity U_{LS} is in between 0.01 and 0.08 m/s (see Table 1).

The results for the mean film thickness δ and the wave velocity C_W are shown in Figs. 11 and 12. As expected from the mass and momentum balances, the mean film thickness δ increases with the liquid superficial velocity U_{LS} , and decreases with the gas superficial velocity U_{GS} . The interfacial velocity C_W in Fig. 12 is calculated using the cross-correlation between the time-signals measured at one reference axial location and at all other axial locations, for the same circumferential position. It was verified that the wave velocity C_W was constant over the length of the sensor and that no dispersion in the roll waves occurred. The measured interfacial velocity C_W corresponds to the characteristic velocity of the roll waves when they exist on the interface, i.e., for all liquid superficial velocities U_{LS} except the lowest one. At the lowest U_{LS} , the Reynolds number Re_{LS} is smaller than the critical one Re_{LS}^{crit} , below

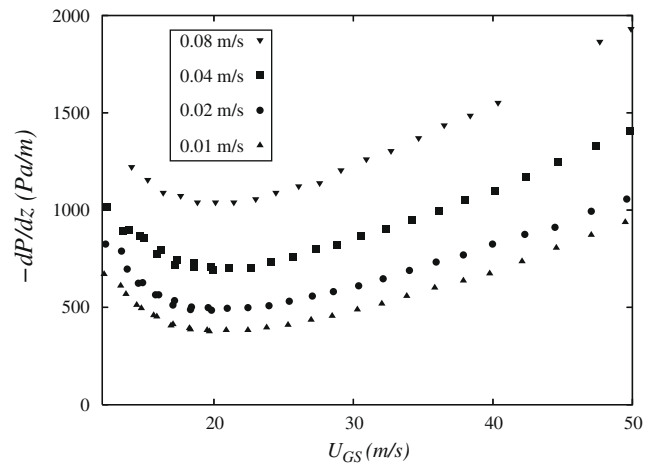


Fig. 10. Mean axial pressure-gradient $-dP/dz$ as a function of the gas superficial velocity U_{GS} , for different liquid superficial velocities U_{LS} .

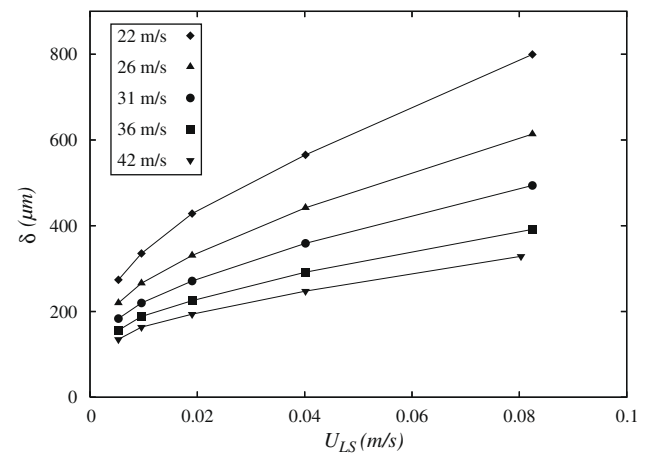


Fig. 11. Mean film thickness δ as a function of the liquid superficial velocity U_{LS} , for different gas superficial velocities U_{GS} .

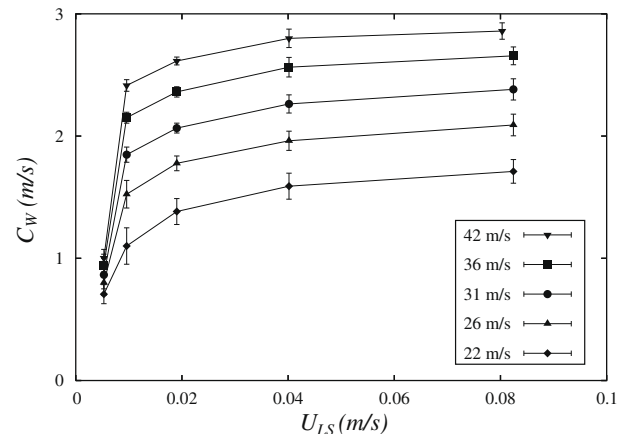


Fig. 12. Mean interfacial velocity C_W as a function of the liquid superficial velocity U_{LS} , for different gas superficial velocities U_{GS} . The error bars correspond to once the standard deviation of the interfacial velocity.

which roll waves do not occur (see Azzopardi, 1997). For the study here, the data for which Re_{LS} is lower than the critical value are not considered. Fig. 12 shows that the interfacial velocity C_W tends to

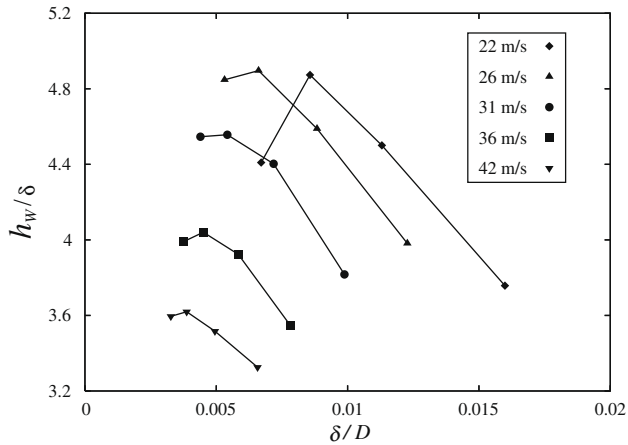


Fig. 13. Ratio of the height of the waves h_w to the mean film thickness δ in the experiments. Each line connecting the dots corresponds to one superficial gas velocity U_{CS} . The velocities near the dots indicate the values of U_{CS} .

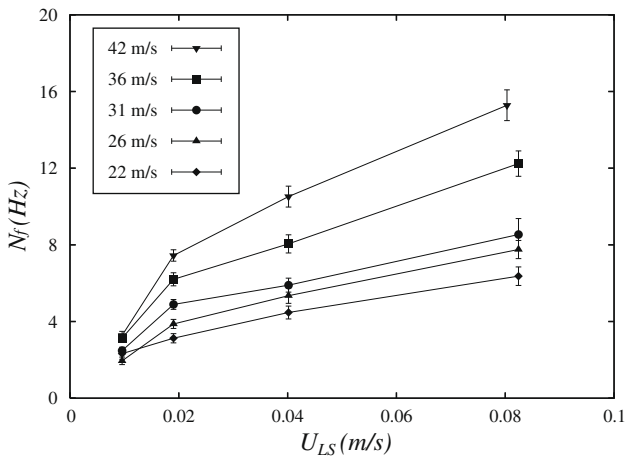


Fig. 14. Mean frequency of the roll waves N_f , as a function of the liquid superficial velocity U_{LS} , for different superficial gas velocities U_{CS} . The error bars correspond to once the standard deviation.

an asymptotic value when the liquid superficial velocity U_{LS} increases, i.e., when the mean film thickness δ increases. In between the two lowest liquid superficial velocities U_{LS} , the interfacial velocity C_W decreases sharply. This can possibly be explained by a velocity of the roll waves larger than that of the base film, and by the absence of roll waves for the lowest superficial velocity. The interfacial velocity C_W increases quite linearly with the superficial gas velocity U_{CS} .

For the roll waves, a robust procedure is needed for their identification in the signal, in order to obtain unbiased statistics. The procedure is described in detail in Belt (2007). It was verified in the experiments that the distribution of the roll waves in space is random (see Belt, 2007; Belt et al., 2007, submitted for publication), which makes the theory for K-type of roughness valid. For the determination of the solidity λ , we need the height h_w , the frequency N_f and the velocity C_W of the roll waves. The velocity C_W and height h_w are shown in Figs. 12 and 13, respectively. The frequency of the roll waves is shown in Fig. 14. It was obtained by counting the roll waves in the time signal, and agrees well with the spectral information of the time signal.

References

- Asali, J.C., Hanratty, T.J., Andreussi, P., 1985. Interfacial drag and film height for vertical annular flow. *AIChE J.* 31, 895–902.
- Azzopardi, B.J., 1997. Drops in annular two-phase flow. *Int. J. Multiphase Flow* 23 (Suppl.), 1–53.
- Belt, R.J., 2007. On the liquid film in inclined annular flow. Ph.D. Thesis, Delft University of Technology.
- Belt, R.J., Van't Westende, J.M.C., Portela, L.M., Prasser, H.M., Mudde, R.F., Oliemans, R.V.A., 2007. Interfacial waves and shear-stress in vertical upward annular flow. In: S5-Thu-B-51, Proceedings of the Sixth International Conference on Multiphase Flow, ICMF2007, Leipzig, Germany, July 9–13, 2007.
- Belt, R.J., Van't Westende, J.M.C., Portela, L.M., Prasser, H.M., submitted for publication. Time and spatially resolved measurements of interfacial waves in vertical annular flow. *Int. J. Multiphase Flow*.
- Churchill, S.W., 1977. Friction factor equation spans all fluid-flow regimes. *Chem. Eng.* 84, 91–92.
- Fore, L.B., Dukler, A.E., 1995a. Droplet deposition and momentum transfer in annular flow. *AIChE J.* 41, 2040–2046.
- Fore, L.B., Dukler, A.E., 1995b. The distribution of drop size and velocity in gas-liquid annular flow. *Int. J. Multiphase Flow* 21, 137–149.
- Fore, L.B., Beus, S.G., Bauer, R.C., 2000. Interfacial friction in gas-liquid annular flow: analogies to full and transition roughness. *Int. J. Multiphase Flow* 26, 1755–1769.
- Henstock, W.H., Hanratty, T.J., 1976. The interfacial drag and the height of the wall layer in annular flows. *AIChE J.* 22, 990–1000.
- Jimenez, J., 2004. Turbulent flows over rough walls. *Annu. Rev. Fluid Mech.* 36, 173–196.
- Lopes, J.C.B., Dukler, A.E., 1986. Droplet entrainment in vertical annular flow and its contribution to momentum transfer. *AIChE J.* 32, 1500–1515.
- Pope, S.B., 2000. *Turbulent Flows*. Cambridge University Press.
- Schlichting, H., 1936. Experimentelle Untersuchungen zum Rauigkeitproblem. *Ing. Arch.* 7, 1–34 (Engl. transl. 1937. Experimental investigation of the problem of surface roughness. NACA TM 823).
- Schlichting, H., 1979. *Boundary-Layer Theory*, seventh ed. McGraw-Hill, New York.
- Tillman, W., 1944. Neue Widerstandsmessungen an Oberflächenstörungen in der turbulenten Reibungsschicht. ZWB Unters. Mitteil. 6619 (Engl. transl. 1951. Additional measurements of the drag of surface irregularities in turbulent boundary layers. NACA TM 1299).
- Van't Westende, J.M.C., Kemp, H.K., Belt, R.J., Portela, L.M., Mudde, R.F., Oliemans, R.V.A., 2007. On the role of droplets in cocurrent annular and churn-annular flow. *Int. J. Multiphase Flow* 33, 595–615.
- Wallis, G.B., 1969. *One-dimensional Two-phase Flow*. McGraw-Hill, New York.
- Wolf, A., Jayanti, S., Hewitt, G.F., 2001. Flow development in vertical annular flow. *Chem. Eng. Sci.* 56, 3221–3235.
- Zabaras, G., Dukler, A.E., Moalem-Maron, D., 1986. Vertical upward cocurrent gas-liquid annular flow. *AIChE J.* 32, 829–843.